

Non-integral vortex structures in diffracted light beams

S. Baumann and E.J. Galvez

Department of Physics and Astronomy, Colgate University, 13 Oak Drive, Hamilton, New York
13346, U.S.A.

ABSTRACT

We study the optical fields produced by non-integral binary forked gratings. We analyze experimentally the phase structure of the light beams by interference. We were able to identify individual optical vortices directly by observing the dislocations in the fringe pattern. Our experimental results agree well with of all the generic features predicted by the theoretical model [M.V. Berry, “Optical vortices evolving from helicoidal and fractional phase steps,” *J. Opt. A* **6**, pp. 259–268, 2004.]. Our results underscore the conservation of orbital angular momentum of the light/optical-apparatus system.

Keywords: Singular Optics, Optical Vortices, Laguerre-Gauss Beams, Orbital Angular Momentum, Forked Diffraction

1. INTRODUCTION

Optical vortices are a topic of intense research today. Within the field of singular optics they provide rich new understanding of waves with complex wavefronts. The orbital angular momentum that they possess adds a new fundamental characteristic to light beams. At the quantum level optical vortices provide a rich n -dimensional system in which to encode quantum information. Optical vortices also add the transfer angular momentum to the set of tools that can be used to manipulate matter with light.

Optical vortices can be generated by various means. One involves the use of computer-generated diffraction gratings, which produce optical-vortex-bearing beams in the diffracted orders. Binary amplitude gratings were the first type of gratings to be used.^{1–3} Their versatility and ease of construction make them very popular for research as well as for education.⁴ Their disadvantage is their low efficiency. Since the diffracted energy is spread among the diffracted orders, the efficiency for producing a given order is low. Blazed forked gratings or phase-blazed gratings enabled a more efficient production of beams in the diffracted orders.^{5,6} However, their fabrication is not trivial. The advent of the spatial light modulator has enabled an easier and more efficient generation of these beams via diffraction by use of a phase-encoded pixilated grating controlled by a computer.⁷ Diffraction from forked gratings can also be used for measuring the optical vortex (i.e., the charge) of a light beam.⁸ Optical vortices can also be produced by transmission through a single phase-plate with an axially dependent thickness.⁹

Recent work on optical vortices has involved the study of beams bearing multiple vortices,^{10–12} non-integer vortices,^{9,14–16} and the propagation dynamics of intertwined vortices.^{17,18} These systems are interesting because they reveal properties of the light field that are not immediately obvious from simple observation of complex light patterns.

In this article we investigate beams produced by non-integral binary diffraction gratings. Beams diffracted by gratings with non-integral dislocations produce an interesting pattern of vortices, which as a whole conserve the angular momentum of the light/optical-apparatus. We use binary forked gratings to appreciate the effect of the dislocation on the various diffracted orders. In Sec. 2 of this article we discuss the general principles of diffraction by binary forked gratings, and the methods that we used to diagnose the diffracted beams. In Sec. 3 we present the results of our study of beams diffracted by non-integral forked gratings.

Further author information: (Send correspondence to E.J.G.)
E.J.G.: E-mail: egalvez@mail.colgate.edu, Telephone: 1 315 228 7205
Proceedings of SPIE **6483**, 64830T (2007).

2. FORKED DIFFRACTION

A discussion of the first-order Fraunhofer diffraction from a forked binary grating has been given before.¹⁹ That discussion can be generalized to all diffracted orders leading to an interesting result: if a beam with a topological charge ℓ_{inc} is incident on a forked diffraction grating with topological charge ℓ_{fork} , then the topological charge of the beam in the n -th diffracted order is given by

$$\ell_{\text{diff}} = \ell_{\text{inc}} + n\ell_{\text{fork}}. \quad (1)$$

We can understand this relation qualitatively the following way. A binary forked grating is a computer generated hologram constructed by calculating the interference pattern produced by two beams forming an angle β , one of zero order and another one of order ℓ_{fork} . It is well known that the points (x, y) at the center of the fringes of the grating satisfy¹⁹

$$m = \frac{x}{\lambda} \sin \beta + \frac{\ell_{\text{fork}} \theta}{2\pi}, \quad (2)$$

where m is an integer, and $\theta = \tan^{-1}(y/x)$ is the angle subtended by point (x, y) relative to the horizontal, with point $(0, 0)$ being the center of the grating. The grating has an average fringe separation given by

$$\langle \Delta x \rangle = \frac{\lambda}{\sin \beta}. \quad (3)$$

The modulation of the fringe separation that is typical of forked gratings depends on ℓ_{fork} . Upon illuminating the grating with a beam at normal incidence results in diffracted orders appearing at angles $\sin^{-1}(n\lambda/\langle \Delta x \rangle)$. The wavefront that emerges from the grating in the direction of order n has a phase dislocation given by $n\ell_{\text{fork}}$. If the beam incident on the grating has a topological charge ℓ_{inc} , then the beam reaching the grating openings has a phase that varies with $\ell_{\text{inc}}\theta$. This phase variation at the grating slits adds to the phase generated by the fringe modulation of the grating. Thus, the diffracted beam has a topological charge given by the sum of the two (i.e., Eq. 1). For integral vortices we can understand this equation from a more general perspective: it is a manifestation of conservation of orbital angular momentum. The dislocation of the grating adds a torque $n\ell_{\text{fork}}\hbar$ per photon to the orbital angular momentum of the incident beam, $\ell_{\text{inc}}\hbar$ per photon, to give the diffracted beam its final orbital angular momentum.

In the laboratory we analyzed the phase pattern of the emerging beam by interference with an expanded reference beam. Optical vortices appeared as forks in the fringe pattern.¹² A topological charge can be read from the interference pattern by the fork dislocation in the fringe pattern. This is shown in Fig. 1. When going on a closed path around a phase singularity we count the number fringes gained or lost in the round trip, with fringes advanced in one direction (e.g., right to left) counted oppositely with those advanced in the reverse direction (left to right). The number of fringes gained or lost give the charge of the singularity. A simple rule to follow is that the charge of a single fork is the number of times minus one.

In this work we generated non-integral vortex beams by diffraction off forked binary gratings. Figure 2 shows a schematic of our apparatus. The beam from a HeNe laser was sent through a Mach-Zehnder interferometer.

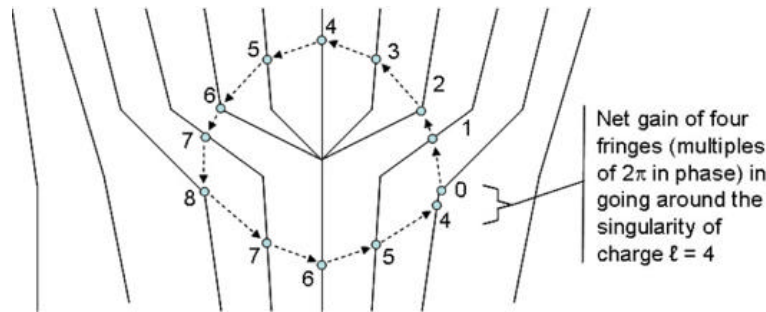


Figure 1. Method to determine the charge of a topological vortex in a fringe pattern. It consists counting the gain or loss of fringes when going in a closed path around the singularity.

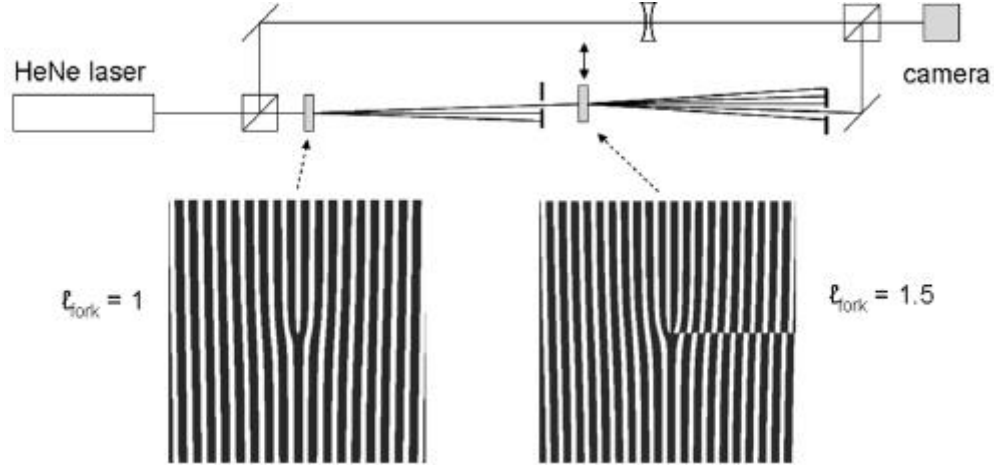


Figure 2. Schematic of the apparatus used to do the experiments. Two forked gratings were used to produce the desired topological charge. Two sample forked gratings are shown. The phase of the resulting beam was analyzed by interference with an expanded zero-order beam.

The beam in one of the arms was incident on a first forked grating. The beam that emerged from the grating was allowed to expand, and all but one of the diffracted orders were stopped by an iris. A second forked grating was aligned in the path of the beam emerging from the iris. The desired diffracted order was allowed to go through a second iris and onto an imaging camera. We investigated the phase of the beam by analyzing the interference pattern produced when the expanded zero-order beam that went through the other arm of the interferometer was allowed to reach the camera.

As a first step toward generating beams with non-integral phase dislocations we verified Eq. 1. Figure 3 shows four interferograms. Frames (a), (b), (c) and (d) correspond respectively to the diffracted orders 2, -2 , -3 and -4 of a beam with $\ell_{inc} = 1$ incident on a grating with $\ell_{fork} = 2$. It can be seen that the charge of the beams in Fig. 3 is in excellent agreement with the value predicted by Eq. 1. The cases shown are just a sample of our studies. In order to do these studies we had to use gratings with slit width-to-separation ratios that did not suppress any of the first four diffracted orders.

3. NON-INTEGRAL VORTEX BEAMS

We can easily produce a non-integral grating by following the prescription demonstrated above but using gratings with a non-integral topological dislocation. It is interesting to ask: What is the resulting pattern? In the

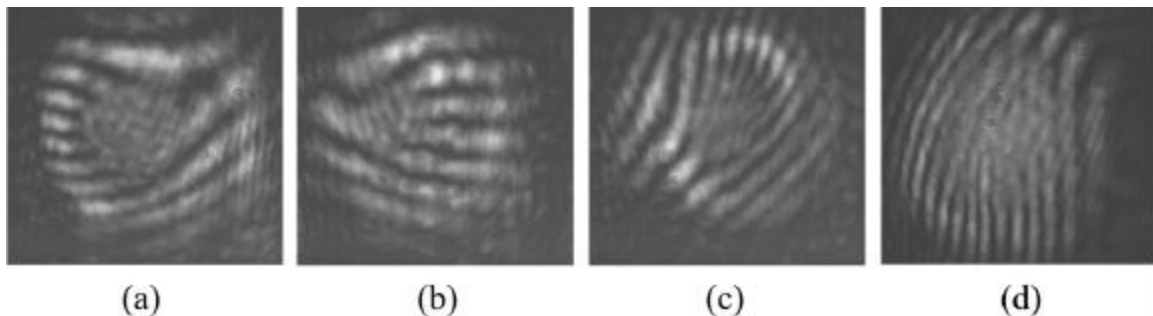


Figure 3. Cases of integral forked diffraction for a beam of topological charge $\ell_{inc} = 1$ incident on a grating with $\ell_{fork} = 2$. The diffracted orders 2, -2 , -3 and -4 , shown in frames (a), (b), (c) and (d), respectively, have topological charges 5, 3, 5 and 7, in agreement with Eq. 1.

theoretical work of Berry¹⁴ and experiments by Leach, Yao and Padgett¹⁵ we learned that rather than generating non-integral phase singularities, the resulting beam contains only integral vortices, arranged in a peculiar way.

We start our study by considering the effect of a non-integral grating on an incident beam. Figure 4 shows images of the beams that result when a zero-order Gaussian beam is diffracted by a non-integral forked grating with $\ell_{\text{fork}} = 1.5$, similar to the one shown in Fig. 2. The top two images of Fig. 4 show the beam profiles of the first (a) and second (b) diffraction orders. A consequence of the non-integral dislocation is an intensity profile in the shape of an open-ring, as seen in frame (a) of Fig. 4. The profile of the beam diffracted in second order is shown in frame (b) of Fig. 4. It has the shape of a closed ring that is typical of an integral vortex beam. According to Eq. 1 the charge of the second diffracted order is $\ell_{\text{diff}} = 3$. Frames (c) and (d) of Fig. 4 show the interference patterns of the beams in frames (a) and (b) of Fig. 4, respectively, with a zero order beam. The pattern for the second order (d) shows a charge-3 fork, consistent with the expectation. The interference pattern of the beam with $\ell_{\text{diff}} = 1.5$ shows one $\ell = 1$ fork in the center of the beam. The pattern is too coarse for us to appreciate well the other phase corrugations, but one can see another phase dislocation along the opening of the open ring.

One of the most interesting aspects of the diffraction off non-integral forked gratings is to observe the formation of the vortices. Below and above the half integral value of ℓ_{fork} the number of vortices in the beam is ℓ_{fork} rounded to the nearest integer. We can see this in Fig. 5. The top row has simulations of the phase of the beams based on Ref. 13. Frames (a), (b), and (c) of Fig. 5 are the simulations for beams with topological charge $7/3$, $7.5/3 = 2.5$ and $8/3$, respectively. Frame (a) of Fig. 5 corresponds to the case when $2 < \ell < 2.5$, where it can be seen that the simulation predicts two vortices in the profile. Vortices can be identified by points where the gray scale goes through the entire range of shades along a loop surrounding the singularity. In the figures they appear at the end of the curves with sharp black/white contrast. Frame (d) of Fig. 5 shows an interferogram of a beam with $\ell = 7/3$ created by second-order diffraction of a beam with $\ell_{\text{inc}} = 1$ incident on a grating with $\ell_{\text{fork}} = 2/3$. The

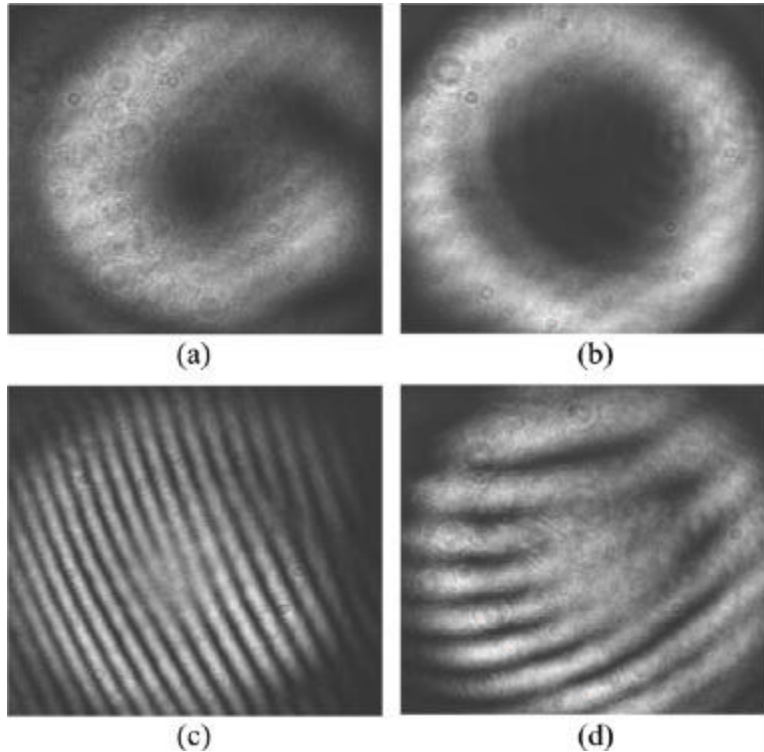


Figure 4. Diffraction off a grating with $\ell_{\text{fork}} = 1.5$ when the incident beam is of order zero. Frames (a) and (b) are the intensity profiles of the first and second diffraction orders, respectively. Frames (c) and (d) are the interference patterns that result between beams (a) and (b), respectively, and an expanded zero-order beam.

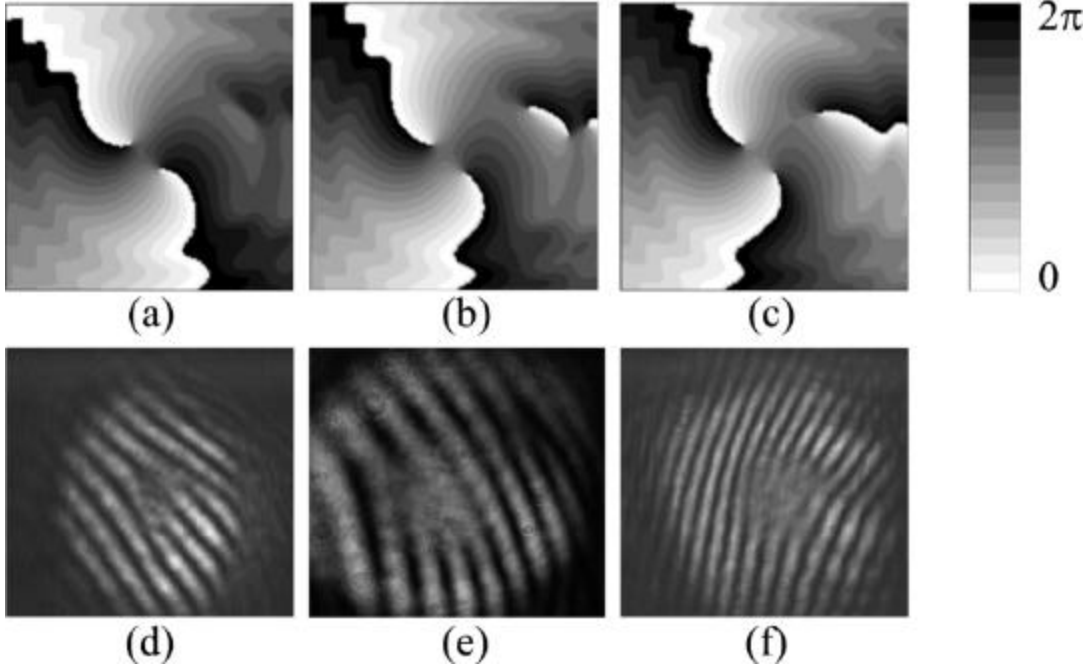


Figure 5. Optical beams with an overall phase dislocation around a half-integer value. Frames a-c show the predictions for the phase of the patterns,¹⁴ with the phase encoded in a gray scale; and d-f show the corresponding experimental measurements of the phase via interferograms. Cases (a,d), (b,e) and (c,f) correspond to beams created by forked gratings with topological charges $7/3$, $7.5/3 = 2.5$ and $8/3$, respectively.

fringe pattern clearly shows two $\ell = 1$ forks in the center of the profile. We get a similar agreement with the case of frames (c) and (f) of Fig. 5. They correspond to the case of a beam with $\ell = 8/3$, where the theory predicts three vortices and the experiment shows a phase dislocation consistent with $\ell = 3$. The beam for case (f) was produced by first-order diffraction of a beam with $\ell_{\text{inc}} = 1$ incident on a grating with $\ell_{\text{fork}} = 5/3$.

For the beam with the half-integer value, $\ell = 2.5$, which is the case of frames (b) and (e) of Fig. 5, the situation is very interesting. The theory predicts two vortices in the central region of the beam and a sequence of $\ell = 1$ vortices of alternating sign on the side of the beam corresponding to the phase discontinuity in the forked grating (i.e., like the one seen in the second binary grating of Fig. 2). This prediction is not entirely obvious from frame (b) of Fig. 5 because it is zoomed-in to match approximately the experimental scale, shown in frame (e). The latter frame shows the interferogram of a beam generated by a zero-order beam diffracted in first order by a grating with $\ell_{\text{fork}} = 2.5$. It shows an $\ell = 2$ dislocation in the central region plus one and maybe more dislocations toward the edge of the beam on the right. The fringe pattern is rather crude to verify specifically the set of alternating vortices, but it does confirm the central phase dislocation.

In an effort to investigate the predicted sequence of alternating vortices we did high-resolution interferograms of several half integer cases. Frame (a) of Fig. 6 shows a high resolution interferogram of a portion of the beam for the case $\ell = 1.5$. Frame (b) shows a computed contour map of the phase of the wave. Frame (c) shows a magnified copy of the cutout region in frame (a). In frame (b) we show our best estimate of the cutout region. Also shown in frame (c) are sketch drawings of the forks caused by the phase vortices. Forks oriented in opposite directions have topological charges of opposite sign.¹² The two forks on the left are consistent with those of frame (b) of Fig. 4. The gray-scale, and therefore phase, advances clockwise for both. The third dislocation from the left has a sign opposite to the two on the left. This is clear from the orientation of the fork in the interferogram, and from the counter-clockwise advance of the phase in the theoretical model. The four labeled dislocations from right to left are consistent with theory, which predicts a sequence of $\ell = 1$ vortices of alternating sign.¹⁴ We based our determination of the location of the labeled forks by analyzing this and several other interferograms

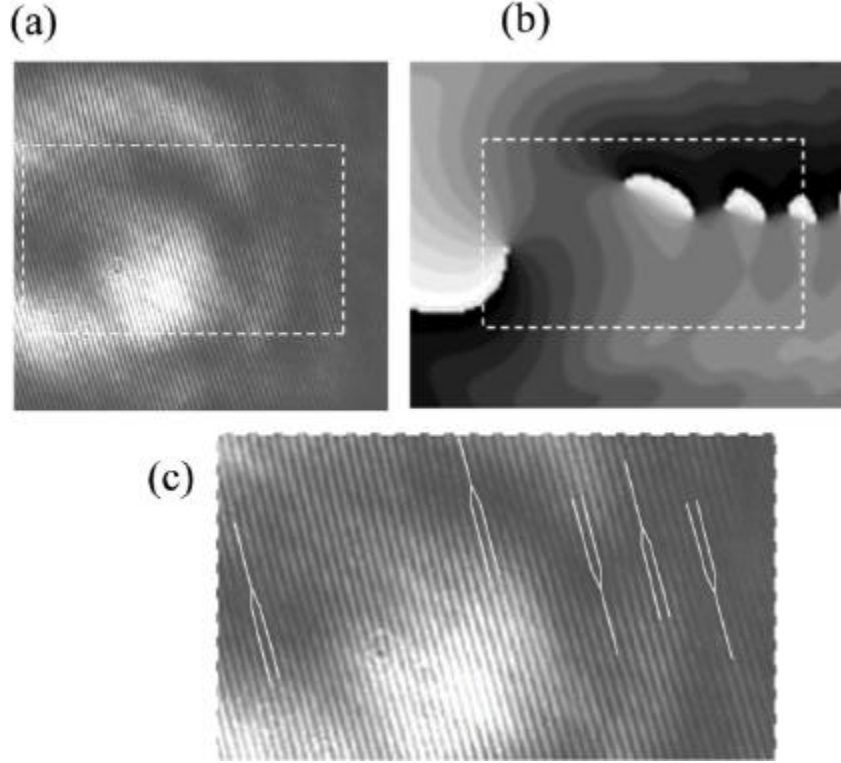


Figure 6. High resolution analysis of the phase structure of the case $\ell = 1.5$. In frame (a) we show a high resolution interferogram. Frame (b) shows the theoretical prediction for the phase of the pattern, and frame (c) shows a blow-up of a region of the interferogram with vortex forks labeled.

of the same case. There appear to be other dislocations beyond the last labeled one on the right of the frame that we could not determine unambiguously. Their determination is difficult because the beam is faint in that region and the alternating forks are separated by one fringe or less. The measured pattern for the case $\ell = 2.5$, not shown here, shows similar features and is consistent with the theoretical model.

Finally, we present one additional comparison and verification of some generic but subtler features of diffraction by non-integral forked gratings. Figure 7 shows a comparison between theoretical predictions of intensity [frame (a)] and phase [frame (b)] for $\ell = 2.5$ with an experimental interferogram at medium fringe resolution [frame (c)]. The main features we wish to focus on are the radial intensity and phase modulations. The radial phase modulations are synchronized with the intensity modulations. The measured intensity modulations show a remarkable similarity with those predicted by the theory. Since the interference fringes of frame (c) of Fig. 7

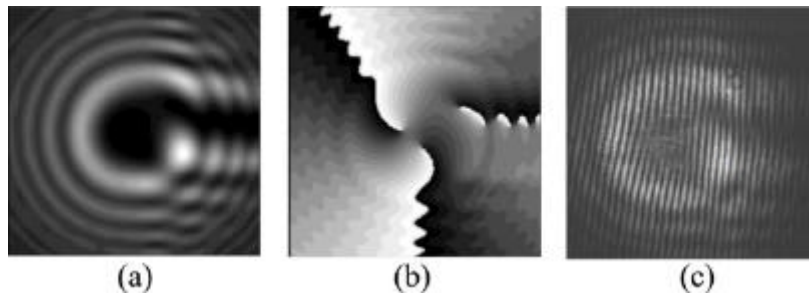


Figure 7. Comparison between theoretical intensity (a) and phase (b) corrugations and the experiment (c) for the case $\ell = 2.5$.

are vertical, those modulations can be seen clearly at points above and below the center of the beam. We refrain of making a more quantitative comparison since the theoretical calculations do not exactly account for the wavefront curvature of signal and reference beams in the experiment. We rather state conservatively that the magnitude of the observed modulations, of the order of a fraction of a fringe are consistent with the theory.

4. CONCLUSIONS

In conclusion, we have investigated the phase and intensity patterns of light beams diffracted by forked diffraction gratings of non-integral charge. The results of the measurements agree well with all the generic phase and intensity patterns predicted by theory.¹⁴ Our measurement method differs from the previous one¹⁵ in that we observe the phase modulations and vortices directly in interferograms. Our measurements confirm the results of the previous work¹⁵ plus add new observations of the intensity modulations that were not clearly visible in that work.

Equation 1 appears to be a general law of conservation of angular momentum of optical beams diffracted by gratings with phase dislocations, where the grating applies a torque on the optical beam such that the diffracted orders emerge with new values of angular momentum. When ℓ_{diff} is an integer the beam is an eigenmode of angular momentum, and thus its angular momentum is proportional to ℓ_{diff} . However, a recent study has shown that in the case of a non-integral value of ℓ_{diff} , the angular momentum of the beam is not proportional to the value of ℓ_{diff} .¹⁵ Thus diffracted beams with overall non-integral topological charge exhibit an interesting richness that deserves further study.

ACKNOWLEDGMENTS

This work was supported by a grant from Research Corporation.

REFERENCES

1. V.Yu. Bazhenov, M.V. Vashnetsov, and M.S. Soskin, "Laser beams with screw dislocations in their wavefronts," *JETP Lett.* **52**, pp. 429–431, 1990.
2. N.R. Heckenberg, R. McDuff, C.P. Smith, and A.G. White, "Generation of optical phase singularities by computer-generated holograms," *Opt. Lett.* **17**, pp. 221–223, 1992.
3. N.R. Heckenberg, R. McDuff, C.P. Smith, H. Rubinsztein-Dunlop, and M.J. Wegener, "Laser beams with phase singularities," *Opt. Quantum Electron.* **24**, pp. S951–S962, 1992.
4. E.J. Galvez, "Gaussian beams in the optics course," *Am. J. Phys.* **74**, pp. 355–361, 2006.
5. H. He, N.R. Heckenberg, and H. Rubinsztein-Dunlop, "Optical particle trapping with higher-order doughnut beams produced using high efficiency computer generated holograms," *J. Mod. Opt.* **42**, pp. 217–223, 1995.
6. G.F. Brand, "The generation of phase singularities at millimetre wavelengths by the use of a blazed grating," *J. Mod. Opt.* **45**, pp. 215–220, 1998.
7. J.E. Curtis and D.E. Grier, "Structure of optical vortices," *Phys. Rev. Lett.* **90**, pp. 1339011–4, 2003.
8. A. Mair, A. Vaziri, G. Welhs, and A. Zeilinger, "Entanglement of the orbital angular momentum states of photons," *Nature* **412**, pp. 313–316, 2001.
9. M.W. Beijersbergen, R.P.C. Coerwinkel, M. Kristensen, and J.P. Woerdman, "Helical-wavefront laser beams produced with a spiral phaseplate," *Opt. Commun.* **112**, pp. 321–327, 1994.
10. G. Molina-Terriza, J.P. Torres, and L. Torner, "Management of the angular momentum of light: Preparation of photons in multidimensional vector states of angular momentum," *Phys. Rev. Lett.* **88**, pp. 0136011–4, 2002.
11. I.D. Maleev and G.A. Swartzlander, Jr., "Composite optical vortices," *J. Opt. Soc. Am. B* **20**, pp. 1169–1176, 2003.
12. E.J. Galvez, N. Smiley, and N. Fernandes, "Composite optical vortices formed by collinear Laguerre-Gauss beams," *Proc. SPIE* **6131**, pp. 19–26, 2006.
13. S.S.R., Oemrawsingh, A. Aiello, E.R. Eliel, G. Nienhuis, and J.P. Woerdman, "How to observe high-dimensional two-photon entanglement with only two detectors," *Phys. Rev. Lett.* **92**, pp. 2179011–4, 2004.

14. M.V. Berry, "Optical vortices evolving from helicoidal integer and fractional phase steps," *J. Opt. A* **6**, pp. 259–268, 2004.
15. J. Leach, E. Yao, and M.J. Padgett, "Observation of the vortex structure of a non-integer vortex beam," *New J. Phys.* **6**, pp. 1–8, 2004.
16. I.V. Basistiy, V.A. Pas'ko, V.V. Slyusar, M.S. Soskin, "Synthesis and analysis of optical vortices with fractional topological charges," *J. Opt. A* **6**, pp. S166–S169, 2004.
17. M.V. Berry and M.R. Dennis, "Knotting and unknotting of phase singularities: Helmholtz waves, paraxial waves and waves in 2+1 spacetime," *J. Phys. A* **34**, pp. 8877–8888, 2001.
18. J. Leach, M.R. Dennis, J. Courtial, and M.J. Padgett, "Vortex knots in light," *New J. Phys.* **7**, pp. 1–11, 2005.
19. G.F. Brand, "Phase singularities in beams," *Am. J. Phys.* **67**, pp. 55–60, 1999.